Final Draft
of the original manuscript:

Starykevich, M.; Salak, A.N.; Zheludkevich, M.L.; Ferreira, M.G.S.:
Modification of Porous Titania Templates for Uniform Metal Electrodeposition from Deep Eutectic Solvent
In: Journal of the Electrochemical Society (2017) Electrochemical Society

DOI: 10.1149/2.1481706jes

Modification of porous titania templates for uniform metal electrodeposition from deep eutectic solvent

M. Starykevich[1], A.N. Salak[1], M.L. Zheludkevich[1,2], M.G.S. Ferreira[1,*]

[1]*Department of Materials and Ceramic Engineering, CICECO-Aveiro Institute of Materials, University of Aveiro, 3810-193 Aveiro, Portugal*

[2]*Institute of Materials Research, Helmholtz-Zentrum Geesthacht, 21502 Geesthacht, Germany*

Abstract

Zinc electrochemical deposition in porous anodic titania from 0.5M $ZnCl_2$ solution in choline chloride based deep eutectic solvent is reported. Electroreduction is performed by a pulse method in titanium dioxide templates modified in three different ways. Titania nanotubes were formed in ethylene glycol based electrolyte with 0,38% (wt.) ammonium fluoride and 1,79% (wt.) of water. The first template has been used as-prepared, without any modification. Such a matrix shows a low fill-factor and zinc electrodeposition mainly occurs on the top of the tubes. The next template was annealed at 450^{o}C to complete crystallization of titania. It results in electrodeposition of zinc along the entire tube surface and consequently in formation of coaxial structure. The third template was modified based on selective crystallization of the pore bottoms using higher anodisation voltage (80 V) than the one used for tubes formation (40 V) in sulphuric acid electrolyte. The successful bottom-up filling of the titania nanotubes is demonstrated in this case. Investigation of the tubes filling is performed by a set of complementary techniques such as GDOES, SEM and TEM.

Keywords: Titanium dioxide, deep eutectic solvent, ionic liquids, electrodeposition, zinc, choline chloride.

Introduction

Recently, porous anodic films on valve metals such as aluminium[1], zirconium[2, 3], iron[4], titanium[3, 5] *etc.*, attract great attention due to wide range of applications. One of the most important uses of the templates is electroformation of nanorods[6] and nanowires. The parameters

* Corresponding author. Tel.: +351 234370354
E-mail address: mgferreira@ua.pt (M.G.S. Ferreira)

of matrix such as length and diameter of the pores, wall thickness can be easily controlled [7] by composition of the anodisation solution [8-11], its temperature[12, 13] or the applied voltage[14, 15].

Titanium dioxide has semiconductive properties that advantageously differentiate it from many other porous anodic layers. Additionally, it reveals common porous anodic template characteristics such as high regularity, homogeneity of the layer *etc*. However, there is scant work on application of porous anodic titania (PAT) as a matrix for electropreparation of metallic or other conductive nanowires, when compared with a growing number of existing studies of the "sister material" porous alumina. Moreover, the majority of both templates studies was performed with detached oxide template instead having them attached to the metal electrode[16-19]. The use of the detached template leads to increase of cost and time due to the additional step of substrate removal and evaporation of an electrical contact. There were several attempts to perform deposition directly in the pores without removing the original substrate. Macak *et al* [20] have reported increasing the conductivity of the bottom part of the tubes via proton intercalation ($Ti^{4+} + e^- + H^+ = Ti^{3+}H^+$).

Porous titania template can be formed in a number of inorganic solutions containing sulphate[21], phosphate[10, 22], acetate[23] ions *etc*. or in organic solutions [5] which are based on glycerol[15], ethylene glycol *etc*. The presence of fluoride ions is mandatory for all these electrolytes, otherwise a dense oxide layer will form instead of a porous one. In the current work we have used ethylene glycol based electrolyte for formation of the pores with several micrometres length and with very smooth walls.

Electrodeposition of active metals from water based solutions is difficult or even impossible. Ionic liquids are promising electrolytes in this area, because they demonstrate unique properties such as wide electrochemical window, high thermal stability, conductivity, negligible vapour pressure, *etc*[24]. High price and water sensitivity are the biggest disadvantages of classical ionic liquids. Deep eutectic solvents[25] (DES) are a cheap alternative to common ionic liquids with similar physicochemical properties. DES are non-toxic, water-/air- stable and also have good potential to be scaled up to industrial level [25]. Choline chloride based DES is one of the alternative green solvents. Several groups have studied in detail the properties of the choline chloride DES. Abbott et al. has studied viscosity and conductivity[26, 27] and influence of different hydrogen bond donors[28, 29]. Moreover, electrodeposition of different metals such as zinc [30-36], tin[37], silver[38] and alloys[39] is under intensive investigation.

In our previous works we have studied zinc electrodeposition from choline chloride (ChCl):ethylene glycol (EG) DES on bulk anodic titania [40]. It was found that electrodeposition on a thick titanium dioxide layer occurred faster than on a thin film. Taking into account previous

studies [41] it was suggested that crystallinity of the films formed at higher anodising voltage (and correspondingly thicker ones) is better.

The main aim of present work is the investigation of direct electrodeposition of metallic nanorods from deep eutectic solvent (DES) into porous anodic titania templates directly on the titanium substrate. Until now, there is no report on successful electrodeposition of zinc in PAT template. Zinc was chosen as a model metal to be electrodeposited because it is an attractive metal due to further possibilities to be oxidized leading to semiconductor materials such a zinc oxide, zinc sulphide, zinc selenide, etc. Moreover, the similar approach can be used for electrodeposition of other metals.

2. Experimental

2.1. Materials

Titanium foil of 1 mm thick (99,2%, Alfa Aesar), Nitric acid (68-70%, Alfa Aesar), Hydrofluoric acid (48-51%, Alfa Aesar), Ammonium fluoride (Puriss p.a. Sigma-Aldrich) Ethylene glycol (99,8% anhydrous, Sigma-Aldrich), Choline chloride (>98%, Sigma), Ethanol (absolute anhydrous), Zinc chloride (98+%, Alfa Aesar), Sulphuric acid (95-98%, Alfa Aesar) were used as received. Deionized water was used as solvent.

2.2. Procedures

Coupons of titanium foil (100×5×1 mm) were used as electrode material for sample preparation. The coupons were consequently rinsed with acetone, ethanol, and distilled water and then they were dried in air. Before anodization, the electrodes were chemically polished in a HF:HNO_3 mixture (1:3 by volume) to mirror finish and finally were rinsed with deionized water. A part of their surface was isolated with chemically resistant varnish, giving defined electrode working area of about 1 cm^2.

A Keithley 237 High Voltage Source-Measure Unit was used as a current source for the sample anodizing. Ethylene glycol solution with 0,38% (wt.) ammonium fluoride and 1,79% (wt.) of water was used as electrolyte[42]. The anodization was performed in a potentiostatic mode with an applied voltage of 40 V applied for 1 hour. The counter electrode was a platinum foil. Anodization was carried out in two steps with intermediate removal of the oxide. The voltage and the electrolyte were the same for both steps and duration of the second step was 30 minutes. Removal of the anodic layer after the first step was done by ultra sonication in the distilled water

during 5 minutes. After anodization the electrodes were washed in ethanol and stored in a desiccator for stabilization of the titania layer during 24 hours. Mechanism of pore formation allows preparation of highly-ordered template using the two-step technique [43].

The crystallization was performed in a furnace at 450ºC for 5 hours with 2ºC/min heating and cooling ramps.

Preparation of DES electrolytes and the electrodeposition experiments were carried out in contact with air. The eutectic system was prepared by mixing choline chloride (ChCl) and ethylene glycol (EG) in the molar ratio of 1:2. Anhydrous zinc chloride was added to the DES to obtain a 0.5 M solution, which was heated and kept at 60°C under vacuum for 24 hours. The as-prepared solution (hereafter DES:Zn) was either directly used for electrodeposition or was stored in desiccator over P_2O_5.

Electrodeposition was performed using a Bio-Logic SAS SP-300 potentiostat. All measurements were done in a Faraday cage. A three-electrode cell consisting of a platinum wire as a reference electrode, graphite rod as a counter electrode and titanium template as a working electrode was used in the experiments. All electrodes after deposition were rinsed in distilled water and then were stored in deionized water for several hours for physically adsorbed zinc species removal.

Investigation of the electrode surface morphology and elemental analysis was performed using a Hitachi SU-70 scanning electron microscope (SEM) coupled with an energy dispersive spectroscope (EDS). A Hitachi 9100 transmission electron microscope (TEM) with acceleration voltage 300kV was also used for the analysis.

The thickness of the layers was estimated by Glow Discharge Optical Emission Spectroscopy (GDOES). GDOES depth profile analysis of the coatings was done using a HORIBA GD-Profiler 2 with a copper anode of 4 mm in diameter. Argon sputtering of the sample surface occurred at a pressure of 650 Pa and power of 30 W. Plasma polishing was performed at a pressure of 900 Pa and power of 10 W. About 1 μm of the porous template have been removed during plasma polishing.

3. Results and discussion

Typical SEM image of porous anodic titania template after anodisation at the conditions indicated in *Experimental* is presented in Fig. 1a. An uniform porous layer is self-aligned and well-ordered forming tapered tubes array, wider at the top [44, 45]. It is also evident that the pores are open on the top. Diameter of the pores and wall thickness on the interface after 0.5 hour of anodisation are about 70 and 30 nm respectively. The thickness of the porous layer is in the range

of 3-3.5 μm as shown in Fig. 1b. The tubes have a smooth wall morphology typical for the anodic layers grown in organic electrolytes[46]. Qualitative GDOES profile of the tubes is presented in fig. 1c. There are two regions which belong to porous titania layer and titanium substrate. After initiating sputtering the titanium and oxygen signals reach a plateau which corresponds to the porous titania part. The second region with the maximal titanium signal intensity and oxygen background level has been reached at the end of sputtering. It corresponds to metallic titanium (substrate) sputtering. The porous film has homogeneous composition along the entire length of the tubes.

Figure 2 depicts TEM image of the porous titania layer with the barrier film on the bottom which was formed during anodization. It can be seen that the pores are closed by titania from the bottom. This compact layer on the pore bottom is named in literature barrier layer and its formation is typical for valve metals such as tungsten, aluminium *etc* [47]. In contrast to the majority of other barrier layers titanium dioxide is a semiconductor. Comparatively the high conductivity of the titania barrier layer facilitates the filling of the porous template. On the other hand, conductivity of the titanium dioxide is also a weakness of this template, because the deposition can occur not only on the bottom but also on the pore walls and on the electrode surface. The Zn electrodeposition experiments were performed using the titania templates described above. Electrical parameters such as current profile and current distribution affect the quantity of reduced zinc at the interface and the uniformity of the deposition process. Optimal results were obtained with a pulsed technique at a current density of 100 mA/cm^2 (current applied in one step). Cathodic and anodic rectangular pulses with a dwell time of 10 μs and 2 μs, respectively, and the same absolute value of current density were applied sequentially. One cycle was applied every second. Anodic current is needed to remove metallic zinc from the electrode interface and opens access to the fresh electrolyte inside the pores. Moreover, a positive potential promotes electromigration of negatively charged zinc species ($ZnCl_3^-$, $Zn_2Cl_5^-$ [32, 39]) inside the tubes. Enrichment of the electrolyte in zinc species also occurs during intervals between the pulses. The relatively long waiting time between the pulses was chosen to allow partial relaxation of the system taking into account the length of the pores and high viscosity of the electrolyte.

3.1 Electrodeposition in as-prepared PAT

The inset in Figure 2 presents an electron diffraction image of as-prepared titanium dioxide tubes. Diffuse ring without separate reflections suggests that the as-prepared porous titania layer is amorphous. The conductivity of the amorphous titania is lower than conductivity

of the crystalline titania. This causes difficulties during deposition, but even so in this condition electroreduction occurs.

In this work the filling of the pores along their length was controlled by GDOES technique. The elemental depth profile of the sample obtained after one hour of deposition in as-prepared template is presented in figure 3a. The position of the interface between the porous titania and substrate was assessed through Ti profile. Zinc signal has very high intensity in the beginning of the electrode sputtering, but it is followed by a sharp decrease. It is evident that the zinc layer was formed mainly on the top of the pores with only minor penetration into pores. The zinc signal goes down to the background at the titania/titanium interface that means almost no zinc deposition occurs at the pores bottom.

This result was confirmed by the electron microscopy as well. Figure 4a depicts a top view of the porous template after 1 hour of deposition. The upper part of the template (around 1 μm here and after) was removed by soft plasma polishing using the GDOES equipment. The pores fill-factor (ratio between the numbers of filled pores to the total number) at this depth is very low, about 5-10%, and decreases closer to the bottom (GDOES results). Additional STEM investigation (fig. 4b) demonstrates that the pores, besides being covered by the zinc layer on the top, are also sealed in random places as it is schematically demonstrated in figure 3b. Sealing the pores at the middle blocks the access of fresh electrolyte and impairs their filling. Changing the electrodeposition parameters does not solve this issue. Therefore, the next step was to modify the template in order to improve the electrodeposition inside the pores.

3.2 Electrodeposition in annealed PAT

Increase of the conductivity of the porous titania template achieved via annealing in air at 450^{o}C. In these conditions the amorphous titania converts into anatase phase that leading to increase of electrical conductivity and, as a result, to more uniform electrodeposition along the whole pore surface. Figure 5 depicts TEM micrograph of porous titania film after annealing. Electron diffraction pattern (insert in figure 5) demonstrates discrete rings with bright spots and it indicates the anatase crystalline structure.

Electrodeposition of zinc was performed at the same conditions as those applied in the as-prepared template. GDOES profile for such sample is presented in figure 6a. Only one titanium profile is shown because of similarity of templates. With the help of this profile the transition from anodic titania to titanium has been demonstrated. The depth profiles for Zn is also presented for two different electrodeposition times, namely 1 hour and 10 minutes. The zinc signal after one hour of deposition in annealed template has a peak in the beginning of sputtering, and then

it decreases and reaches a plateau followed by a second decrease until the background level at the titania/titanium interface. The template can be divided in three main zones according to the shape of the zinc signal curve. The first zone, in the beginning of sputtering, is the electrode surface and it has a high zinc signal because of a deposit formed on the electrode surface. The middle part of the template (zone II) shows a plateau which means that pores are successfully and homogeneously filled along the length. Then, near the interface between the anodic film and substrate (zone III), a small zinc peak appears and it can be explained by the presence of empty space next to the bottom as schematically shown in figure 6b. This irregularity forms due to strong diffusion limitation, which originates concentration gradient of zinc species and consequently results in different zinc deposition rate along the length of pores. The faster deposition rate on the wall surface at the pore opening leads to the situation that after a certain time the pore fully closes leaving a void with entrapped electrolyte closer to the pore bottom. High homogeneity (geometrical shape and distribution) of the tubes ensures sealing of the pores mainly at specific depth depending on solution concentration, pore length and diameter. A noteworthy detail is that regular sealing (at the same distance from the surface) is only possible if growth occurs through the whole length of the tube simultaneously, otherwise the pores close randomly as it was shown for the as-prepared templates.

Analysing the depth profiles after shorter deposition times can provide important information on the kinetics of pore filling. The profile after 10 minutes was chosen since this time ensures a detectable signal, but at the same time the sealing doesn’t occur yet (green curve in figure 6a). The zinc signal reaches a plateau at the beginning of sputtering and remains at the same level until pore bottoms are reached. It is reasonable to suggest that, in this zone, the walls of the pores are homogeneously covered with a thin layer of zinc as schematically represented in figure 6c. The peak on the zinc signal appears near the titania/titanium interface presumably because the higher quantity of zinc deposited in this plane.

In support of GDOES results, SEM studies were also performed. Figure 7 demonstrates templates surfaces after 1 hour and after 10 minutes of deposition (GDOES polishing was also carried out). Zinc nanowires inside the template are clearly seen after 1 hour of deposition (fig. 7a). The fill-factor at this plane is near 90% which is much higher than in the as-prepared templates. The SEM image after a short-time deposition indicates formation of zinc precipitates on the tubes walls (fig. 7b).

Based on both GDOES measurements (1 hour and 10 minutes) and SEM results we suggest that zinc deposition occurs simultaneously on the whole titania surface and in the beginning of growth zinc forms coaxial tubes (titania outer layer and zinc inner). Longer

deposition leads to sealing the tubes and filling of the template from these seals until interface (fig 6b).

3.3 Electrodeposition in PAT after bottom crystallization.

As it was shown above, electrodeposition in the as-prepared and in the annealed templates occurs on the whole tube length. Based on this result one can assume that bottom-up filling of the tubes requires higher conductivity of the bottom of the pores compared to the walls. One of the ways to create different conductivity is selective crystallisation. Fortunately, during the pores preparation process, current passes mostly through the bottom of the tubes [45]. It makes possible a selective electrochemical modification of pore bottom without strong effect on the walls.

Influence of the anodisation parameters on crystallinity of the titania was demonstrated by Shibata, Zhu[41] and Xing *et al.*[48]. The authors showed that dense anodic titania films prepared at higher anodisation voltage [41] and at longer anodisation time [48] had better crystallinity. Additionally, it was shown in our recent paper [40] that zinc electrodeposition rate raises with increasing the titania barrier layer thickness. At the same time, the thickness of the anodic barrier layer depends on the oxidation voltage and becomes bigger at higher potential. Therefore, an additional anodisation step was applied to the as-prepared template. The treatment of the prepared template was done in a 1M sulphuric acid in two steps. The solution and procedure of anodisation were the same as those used in our previous work where the compact anodic titania films were studied [40]. The first step was performed in galvanostatic mode at 10 mA/cm^2. The second step took place in potentiostatic mode at 80 V during 2.5 hours. Galvanostatic mode was changed to potentiostatic one when the potential reached 80 V. The anodisation voltage at this process is two times higher than template formation voltage (40 V) that, together with long oxidation time, results in thicker and better crystallized barrier layer in comparison with that in the as-prepared template.

Effect of such an additional anodisation on the template structure was analysed by TEM. Regular porous structure with relatively thick barrier layer on the bottom (compared to the as-prepared template, fig. 2) is seen in figure 8a. Moreover, the selected area electron diffraction shows significant difference in crystallinity of the anodic titania at walls and barrier parts. The diffraction pattern of walls does not represent separate reflections indicating that the material is amorphous (fig. 8b). Nevertheless, at the diffraction pattern from the barrier layer shows rings, which confirm the polycrystalline structure of this area (fig, 8c). The reflections are not sharp due to very small size of the crystallites.

Zinc deposition in the template after crystallisation of the barrier layer was performed at the same condition as in two cases described above. The GDOES results obtained on this specimen are presented in figure 9. Zinc signal after 1 hour of deposition has a high intensity in the beginning of sputtering, afterward the intensity slowly decreases until the template bottom is reached. The amount of zinc is comparatively high along the whole length of titania pores, and in this way the filling of the pores had to start from the bottom. A gradual decrease of the zinc signal happens because the template is imperfect. Although reduction occurs mainly on the bottom part there is also some deposition simultaneously on the walls (although in a far less degree than in the case of the as-prepared template).

An additional proof of the suggested mechanism of pore filling can be obtained after analysis of the electrode prepared after 10 minutes of deposition (fig. 9a, green line). Zinc signal has a peak close to the bottom and almost background signal in the beginning of sputtering. This difference of the zinc signal is explained by a small amount of zinc which was deposited at different parts of the tubes. Filling of the tubes after 1 hour and after 10 minutes of deposition are presented schematically in figure 9 b and c correspondingly.

It is evident from SEM image and agrees with GDOES results that most of the pores are filled by secondary material (fig. 10a). Besides, the fill-factor is about 90% that is much higher than that in the case of the as-prepared template. The STEM image presented in figure 10b demonstrates homogeneous pores filling. EDX spectrum shows four elements (fig. 10c): titanium, oxygen, zinc and copper indicating that porous anodic titania (Ti, O) was successfully filled by zinc as a secondary material. The copper signal comes from a TEM grid.

4. Conclusions

Electrodeposition of zinc from a 0.5M $ZnCl_2$ solution in choline chloride/ethylene glycol eutectic solvent in porous anodic titania templates was successfully performed using pulse technique. It was demonstrated that electrodeposition in the as-prepared template occurs in random places without regular pore filling. Annealing of the template at 450^{o}C converts amorphous titania of the as-prepared template to anatase. It improves conductivity of the template along the full length of the pores and allows regular deposition over the whole pore surface. Successful bottom up filling was performed in the template with additional electrocrystallization of the barrier layer.

Acknowledgements

The financial support of the European Commission and Portuguese Foundation for Science and Technology (FCT) in frame of the projects PIRSES-GA-2011-295273 – NANEL and

PTDC/CTM-NAN/113570/2009, respectively, is gratefully acknowledged. M. Starykevich also thanks prof. Patrik Schmuki and Nhat Truong Nguyen (University of Erlangen-Nuremberg) for advising on TEM samples preparation.

Figures.

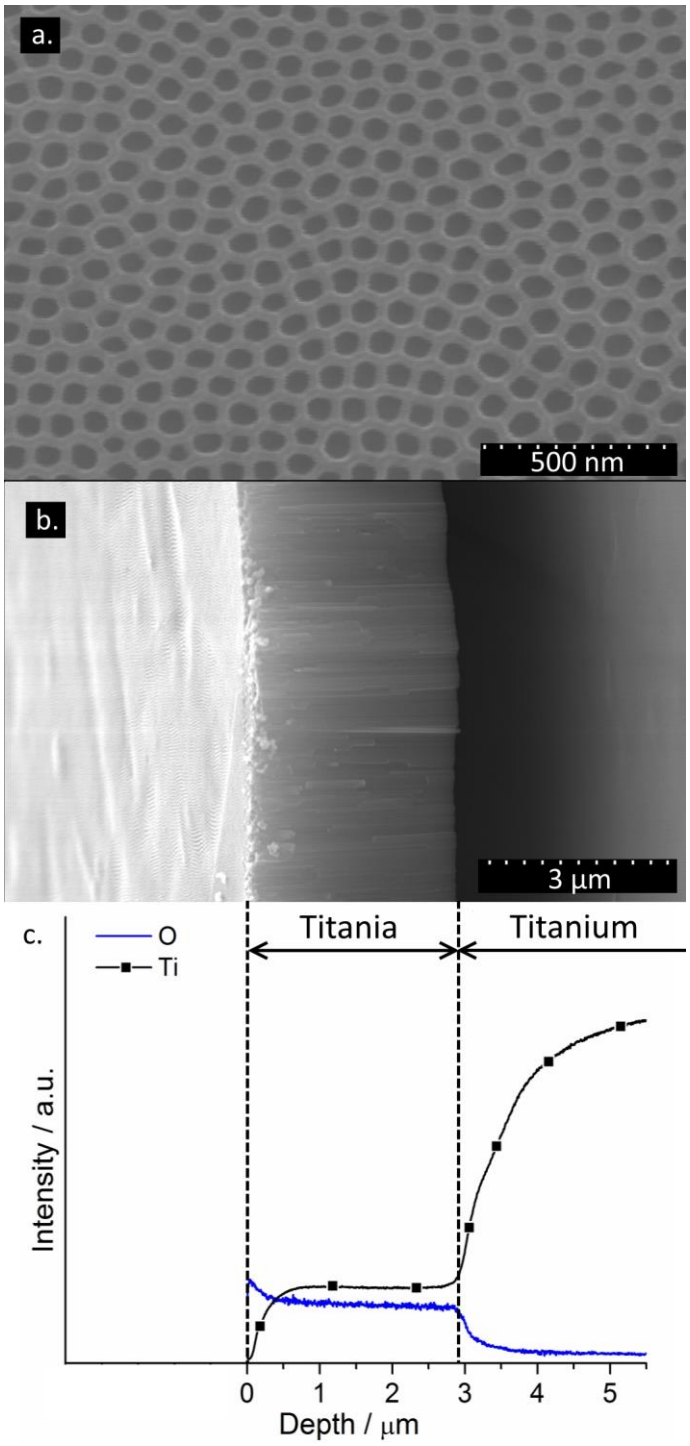

Figure 1. SEM images of the titanium electrode surface (a), cross-section (b) and qualitative GDOES profile (c) obtained on electrode after 30 minutes of anodisation in ethylene glycol ammonium fluoride solution at 40V.

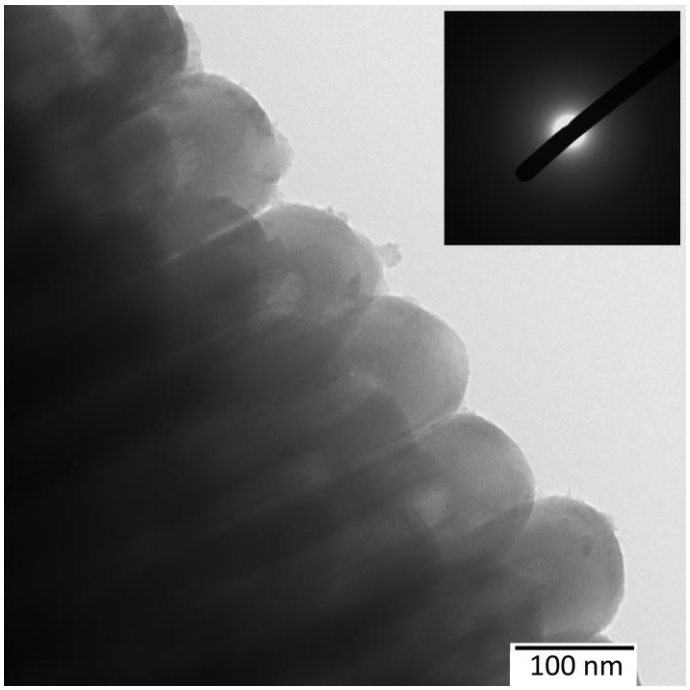

Figure 2. TEM image of as-prepared titanium dioxide tube, the inset shows selected area electron diffraction pattern.

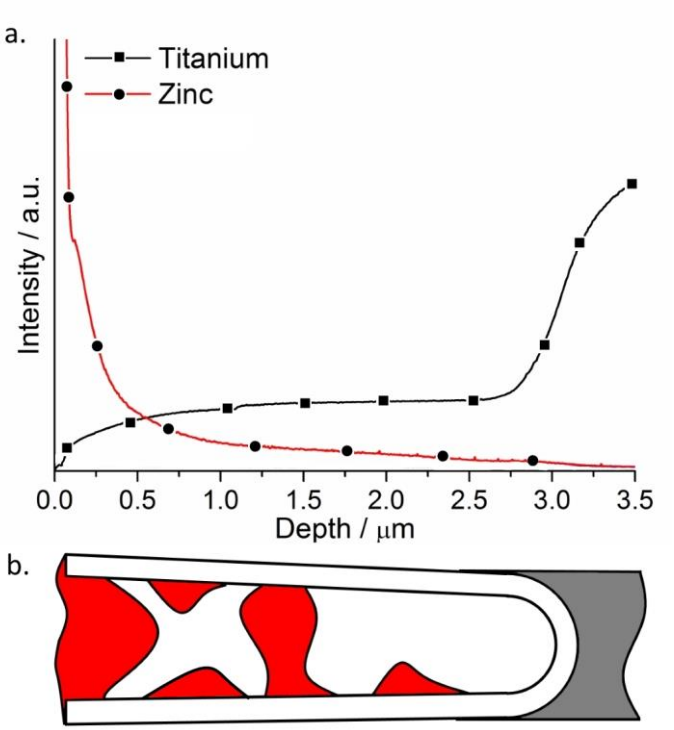

Figure 3. Qualitative depth profile of a porous titanium oxide measured by GDOES after zinc deposition during 1 hour (a) and schematic representation of the pores filling (b).

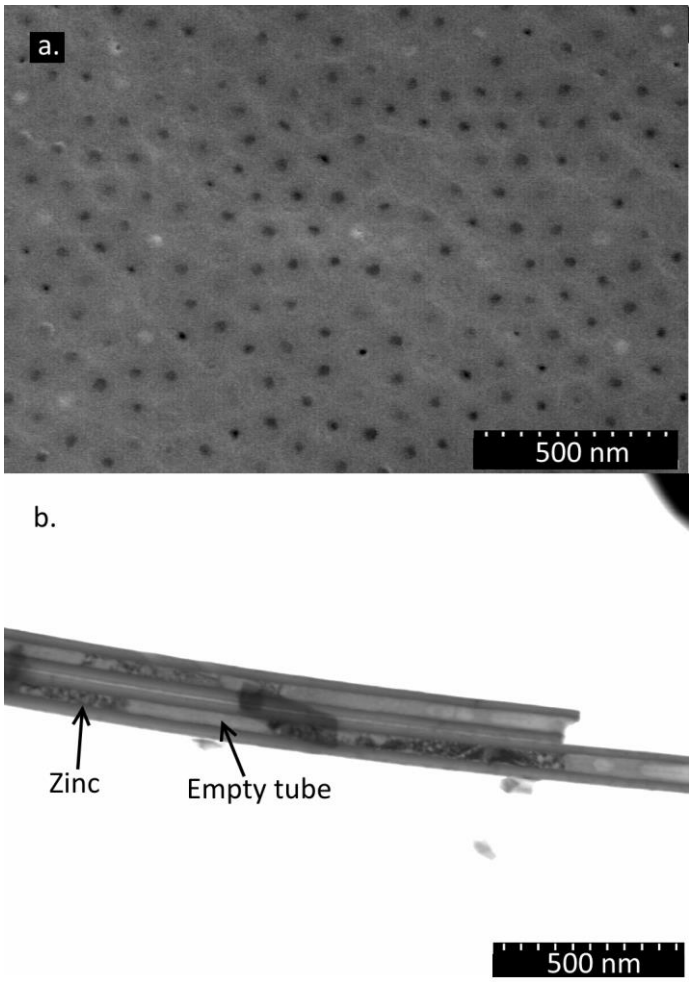

Figure 4. SEM (after plasma polishing) (a) and STEM (b) micrographs obtained after electrodeposition in as-prepared template for 1 hour.

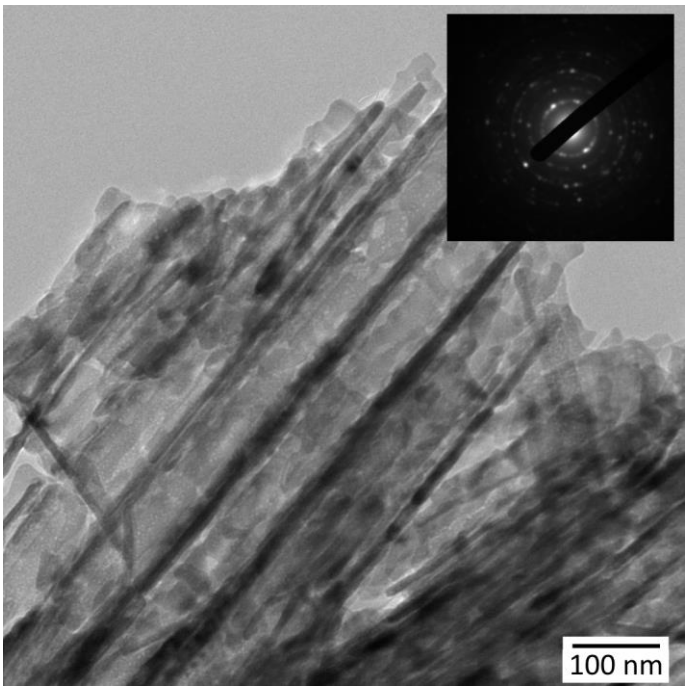

Figure 5. TEM image of annealed titanium dioxide tube, the inset shows selected area electron diffraction pattern.

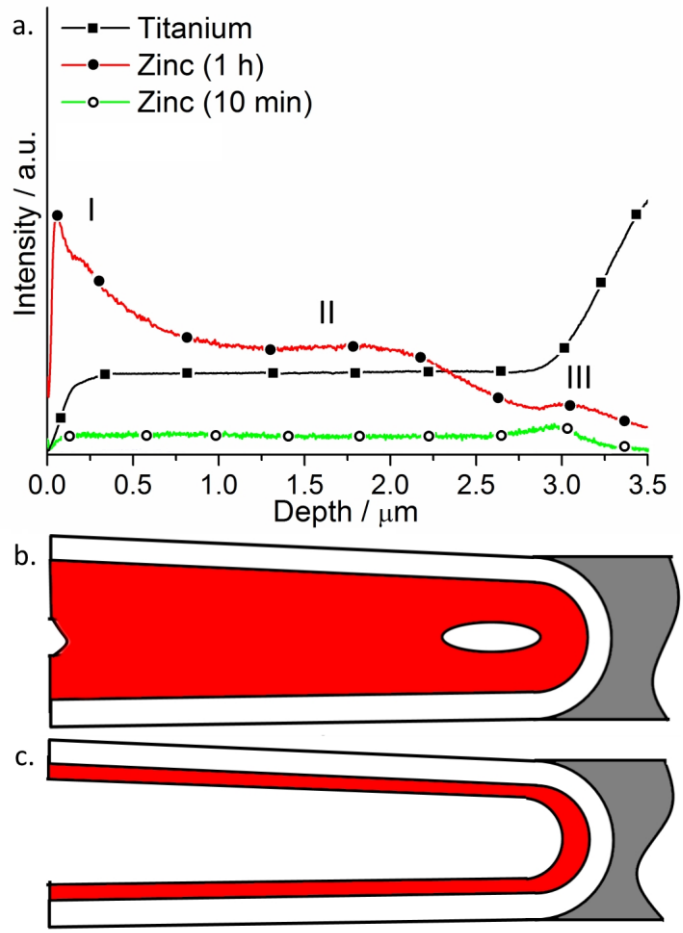

Figure 6. Qualitative depth profile of a porous titanium oxide measured by GDOES after zinc deposition during 10 minutes and 1 hour (a) and schematic representation of the pores filling after 1 hour (b) and 10 minutes (c) of deposition.

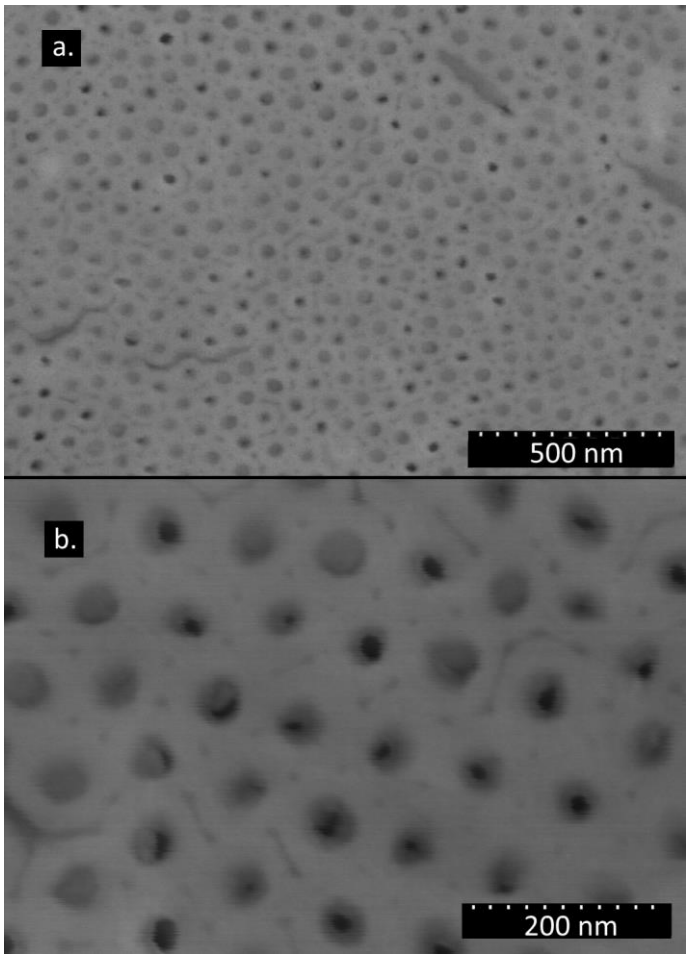

Figure 7. SEM (after plasma polishing) micrographs obtained after electrodeposition in annealed template for 1 hour (a) and 10 minutes (b).

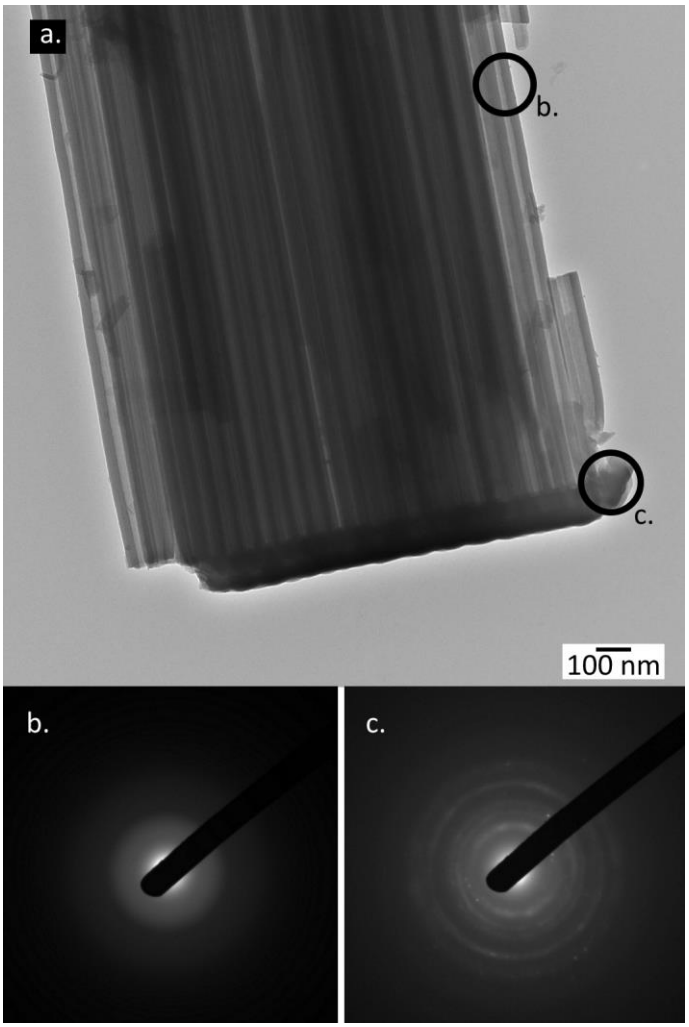

Figure 8. TEM image of titanium dioxide tube after bottom crystallization (a), selected area electron diffraction pattern of the walls (b) and bottom part (c).

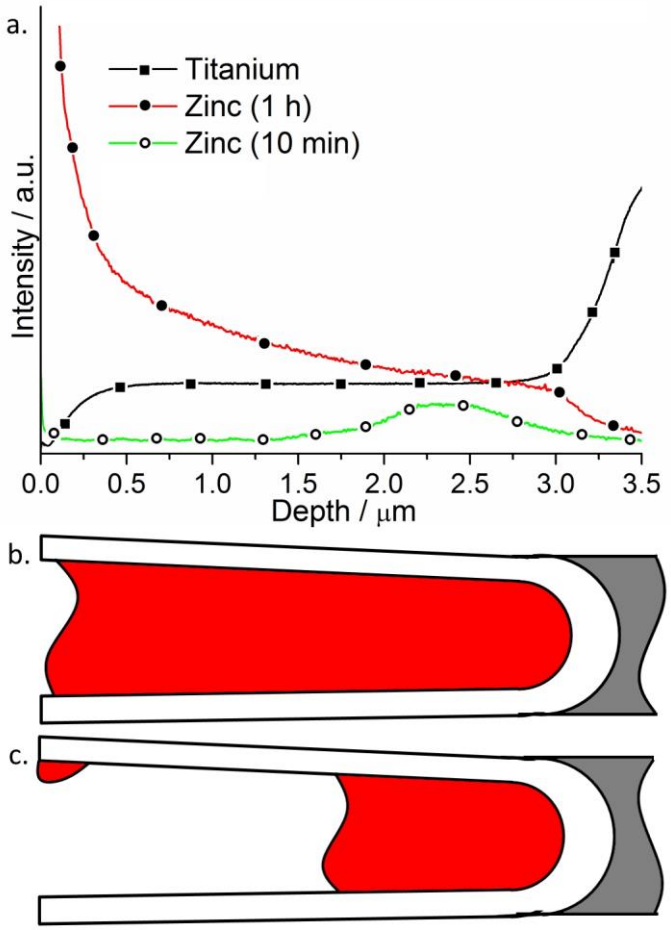

Figure 9. Qualitative depth profile of a porous titanium oxide measured by GDOES after zinc deposition during 10 minutes and 1 hour (a) and schematic representation of the pores filling after 1 hour (b) and 10 minutes (c) of deposition.

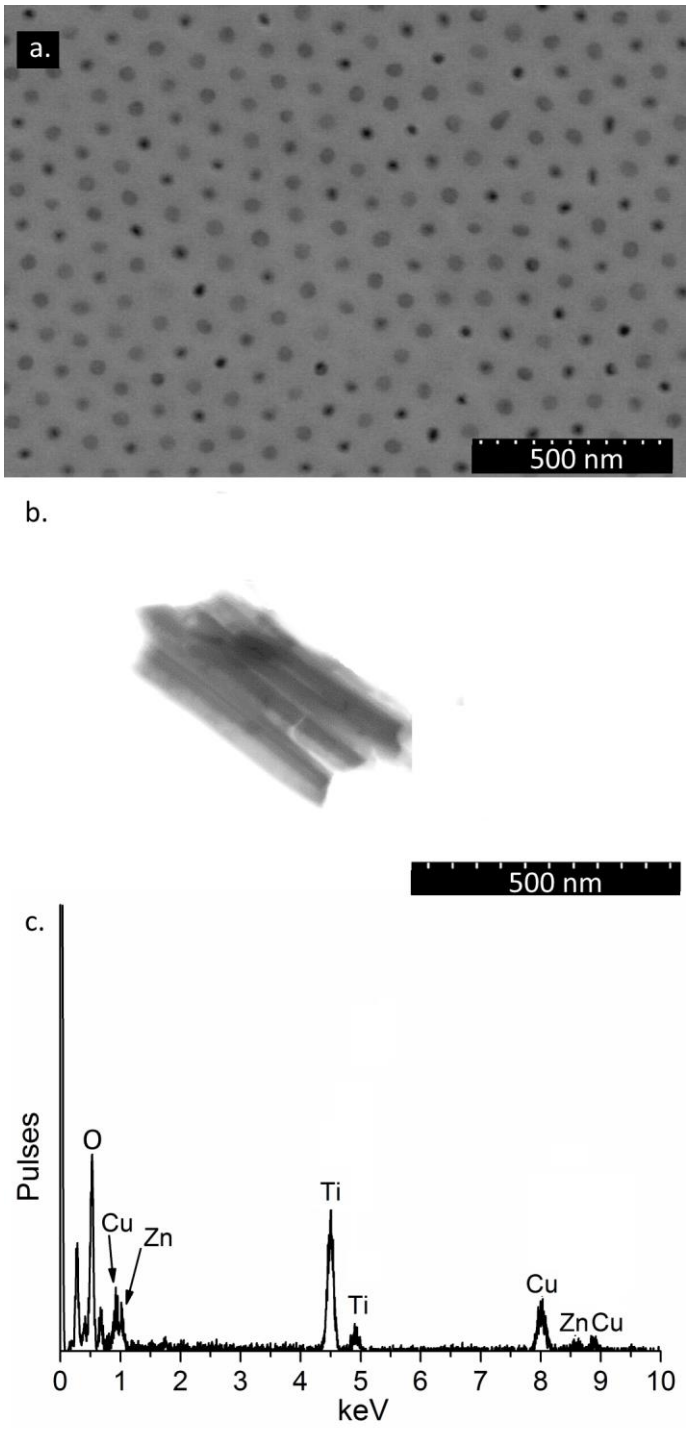

Figure 10. SEM (after plasma polishing) (a) and STEM (b) micrographs obtained after electrodeposition in template after bottom crystallisation for 1 hour. The EDS spectrum recorded after zinc deposition (c).

References

1. R. C. Furneaux, W. R. Rigby, and A. P. Davidson, *Nature*, **337** (6203), 147-149 (1989).
2. S. Berger, F. Jakubka, and P. Schmuki, *Electrochemistry Communications*, **10** (12), 1916-1919 (2008).
3. H. Tsuchiya, J. M. Macak, A. Ghicov, L. Taveira, and P. Schmuki, *Corrosion Science*, **47** (12), 3324-3335 (2005).
4. E. P. Haripriya, K. V. Oomman, P. Maggie, K. M. Gopal, and A. G. Craig, *Nanotechnology*, **17** (17), 4285 (2006).
5. J. M. Macak and P. Schmuki, *Electrochimica Acta*, **52** (3), 1258-1264 (2006).
6. M. Starykevich, A. D. Lisenkov, A. N. Salak, M. G. S. Ferreira, and M. L. Zheludkevich, *ChemElectroChem*, **1** (9), 1484-1487 (2014).
7. D. Kim, F. Schmidt-Stein, R. Hahn, and P. Schmuki, *Electrochemistry Communications*, **10** (7), 1082-1086 (2008).
8. L. Zaraska, G. D. Sulka, and M. Jaskuła, *Journal of Solid State Electrochemistry*, **15** (11), 2427-2436 (2011).
9. A. Elsanousi, J. Zhang, H. M. H. Fadlalla, F. Zhang, H. Wang, X. Ding, Z. Huang, and C. Tang, *Journal of Materials Science*, **43** (22), 7219-7224 (2008).
10. A. Ghicov, H. Tsuchiya, J. M. Macak, and P. Schmuki, *Electrochemistry Communications*, **7** (5), 505-509 (2005).
11. S. Z. Chu, K. Wada, S. Inoue, M. Isogai, Y. Katsuta, and A. Yasumori, *Journal of The Electrochemical Society*, **153** (9), B384-B391 (2006).
12. T. Aerts, T. Dimogerontakis, I. De Graeve, J. Fransaer, and H. Terryn, *Surface and Coatings Technology*, **201** (16–17), 7310-7317 (2007).
13. T. Ruff, R. Hahn, and P. Schmuki, *Applied Surface Science*, **257** (19), 8177-8181 (2011).
14. Y. Ji, K.-C. Lin, H. Zheng, J.-j. Zhu, and A. C. S. Samia, *Electrochemistry Communications*, **13** (9), 1013-1015 (2011).
15. J. M. Macak, H. Hildebrand, U. Marten-Jahns, and P. Schmuki, *Journal of Electroanalytical Chemistry*, **621** (2), 254-266 (2008).
16. D. Fang, K. Huang, S. Liu, and D. Qin, *Electrochemistry Communications*, **11** (4), 901-904 (2009).
17. R. Chen, D. Xu, G. Guo, and L. Gui *Journal of The Electrochemical Society*, **150** (3), G183-G186 (2003).
18. R. Inguanta, M. Butera, C. Sunseri, and S. Piazza, *Applied Surface Science*, **253** (12), 5447-5456 (2007).
19. J. Xu, X. Huang, G. Xie, Y. Fang, and D. Liu, *Materials Research Bulletin*, **39** (6), 811-818 (2004).
20. J. M. Macak, B. G. Gong, M. Hueppe, and P. Schmuki, *Advanced Materials*, **19** (19), 3027-3031 (2007).
21. J. M. Macak, K. Sirotna, and P. Schmuki, *Electrochimica Acta*, **50** (18), 3679-3684 (2005).
22. S. Bauer, S. Kleber, and P. Schmuki, *Electrochemistry Communications*, **8** (8), 1321-1325 (2006).
23. H. Tsuchiya, J. M. Macak, L. Taveira, E. Balaur, A. Ghicov, K. Sirotna, and P. Schmuki, *Electrochemistry Communications*, **7** (6), 576-580 (2005).
24. D. M. F. Endres, A. Abbott, *Electrodeposition from Ionic Liquids*, WILEY-VCH Verlag GmbH & Co. KGaA, Weinheim (2008.).
25. E. L. Smith, A. P. Abbott, and K. S. Ryder, *Chemical Reviews*, **114** (21), 11060-11082 (2014).

26. A. P. Abbott, R. C. Harris, and K. S. Ryder, *The Journal of Physical Chemistry B,* **111** (18), 4910-4913 (2007).
27. A. P. Abbott, *ChemPhysChem,* **6** (12), 2502-2505 (2005).
28. A. P. Abbott, G. Capper, D. L. Davies, R. K. Rasheed, and V. Tambyrajah, *Chemical Communications,* (1), 70-71 (2003).
29. A. P. Abbott, D. Boothby, G. Capper, D. L. Davies, and R. K. Rasheed, *Journal of the American Chemical Society,* **126** (29), 9142-9147 (2004).
30. A. Bakkar and V. Neubert, *Electrochemistry Communications,* **9** (9), 2428-2435 (2007).
31. A. H. Whitehead, M. Pölzler, and B. Gollas, *Journal of The Electrochemical Society,* **157** (6), D328-D334 (2010).
32. A. P. Abbott, J. C. Barron, G. Frisch, S. Gurman, K. S. Ryder, and A. Fernando Silva, *Physical Chemistry Chemical Physics,* **13** (21), 10224-10231 (2011).
33. A. P. Abbott, J. C. Barron, G. Frisch, K. S. Ryder, and A. F. Silva, *Electrochimica Acta,* **56** (14), 5272-5279 (2011).
34. N. M. Pereira, P. M. V. Fernandes, C. M. Pereira, and A. Fernando Silva, *Journal of The Electrochemical Society,* **159** (9), D501-D506 (2012).
35. L. Vieira, R. Schennach, and B. Gollas, *Electrochimica Acta,* **197** 344-352 (2016).
36. L. Vieira, A. H. Whitehead, and B. Gollas, *Journal of The Electrochemical Society,* **161** (1), D7-D13 (2014).
37. S. Salomé, N. M. Pereira, E. S. Ferreira, C. M. Pereira, and A. F. Silva, *Journal of Electroanalytical Chemistry,* **703** (0), 80-87 (2013).
38. A. P. Abbott, K. E. Ttaib, G. Frisch, K. S. Ryder, and D. Weston, *Physical Chemistry Chemical Physics,* **14** (7), 2443-2449 (2012).
39. A. P. Abbott, G. Capper, K. J. McKenzie, and K. S. Ryder, *Journal of Electroanalytical Chemistry,* **599** (2), 288-294 (2007).
40. M. Starykevich, A. N. Salak, D. K. Ivanou, K. A. Yasakau, P. S. André, R. A. S. Ferreira, M. L. Zheludkevich, and M. G. S. Ferreira, *Journal of The Electrochemical Society,* **164** (2), D88-D94 (2017).
41. T. Shibata and Y. C. Zhu, *Corrosion Science,* **37** (2), 253-270 (1995).
42. J. Kapusta-Kołodziej, L. Zaraska, and G. D. Sulka, *Applied Surface Science,* **315** 268-273 (2014).
43. J. M. Macak, S. P. Albu, and P. Schmuki, *physica status solidi (RRL) – Rapid Research Letters,* **1** (5), 181-183 (2007).
44. S. P. Albu, A. Ghicov, S. Aldabergenova, P. Drechsel, D. LeClere, G. E. Thompson, J. M. Macak, and P. Schmuki, *Advanced Materials,* **20** (21), 4135-4139 (2008).
45. S. Berger, J. Kunze, P. Schmuki, A. T. Valota, D. J. LeClere, P. Skeldon, and G. E. Thompson, *Journal of The Electrochemical Society,* **157** (1), C18-C23 (2010).
46. J. M. Macak, H. Tsuchiya, L. Taveira, S. Aldabergerova, and P. Schmuki, *Angewandte Chemie International Edition,* **44** (45), 7463-7465 (2005).
47. A. Michaelis, in *Electrochemical Surface Modification*, p. 1-106, Wiley-VCH Verlag GmbH & Co. KGaA, (2008).
48. J. Xing, Z. Xia, J. Hu, Y. Zhang, and L. Zhong, *Corrosion Science,* **75** 212-219 (2013).